Available online at www.sciencedirect.com
SCIENCE DIRECT
Icarus 181 (2006) 302–308
ICARUS
www.elsevier.com/locate/icarus

Near-infrared spectra of laboratory H_2O–CH_4 ice mixtures

Max P. Bernstein *, Dale P. Cruikshank, Scott A. Sandford

NASA Ames Research Center, MS 245-6, Moffett Field, CA 94035, USA

Received 13 July 2005; revised 17 October 2005

Available online 13 December 2005

Abstract

We present 1.25–19 μm infrared spectra of pure solid CH_4 and $H_2O/CH_4 = 87$, 20, and 3 solid mixtures at temperatures from 15 to 150 K. We compare and contrast the absorptions of CH_4 in solid H_2O with those of pure CH_4. Changes in selected peak positions, profiles, and relative strength with temperature are presented, and absolute strengths for absorptions of CH_4 in solid H_2O are estimated. Using the two largest ($\nu_3 + \nu_4$) and ($\nu_1 + \nu_4$) near-IR absorptions of CH_4 at 2.324 and 2.377 μm (4303 and 4207 cm^{-1}), respectively, as examples, we show that peaks of CH_4 in solid H_2O are at slightly shorter wavelength (higher frequency) and broader than those of pure solid CH_4. With increasing temperature, these peaks shift to higher frequency and become increasingly broad, but this trend is reversible on re-cooling, even though the phase transitions of H_2O are irreversible. It is to be hoped that these observations of changes in the positions, profiles, and relative intensities of CH_4 absorptions with concentration and temperature will be of use in understanding spectra of icy outer Solar System bodies.

Keywords: Ices; Infrared observations; Spectroscopy; Surfaces, planets; Surfaces, satellites

1. Introduction

Infrared (IR) spectra have demonstrated that solid CH_4 is present on a number of outer Solar System objects, including Triton (Cruikshank et al., 1982) and Pluto (Cruikshank et al., 1976), where it is thought to be frozen into N_2 ice (Quirico et al., 1999; Grundy and Buie, 2001), the Kuiper Belt Objects (KBOs) Quaoar (Brown, 2003, and personal communication), 90377 Sedna (Barucci et al., 2005), 2003 UB_{313} (Trujillo et al., 2005; Brown et al., 2005), and FY9 (Barkume et al., 2005), and CH_4 is known to be present in number of comets (Gibb et al., 2003).

Since H_2O is nearly ubiquitous in the outer Solar System (Roush, 2001) CH_4 on icy planetesimals is likely to come into contact with H_2O, potentially changing its spectral properties. Since mathematical addition of spectra of pure materials is not equivalent to the spectra of actual mixtures, fitting CH_4 profiles in spectra of outer Solar System bodies will require lab spectra of solid CH_4 mixed at a molecular level with H_2O at relevant temperatures.

Near-IR spectra of CH_4 as a pure solid and mixed in N_2 have been measured in the lab at various temperatures and concentrations (Quirico and Schmitt, 1997; Grundy et al., 2002). Absolute absorption intensities (*A* values) for near-IR absorptions of pure solid CH_4 were published recently (Gerakines et al., 2005), and real and imaginary indices of refraction (ns and ks) have been determined for both pure methane (Khare et al., 1989; Pearl et al., 1991) and pure H_2O, albeit for just the hexagonal phase (Grundy and Schmitt, 1998). Despite this wealth of beautiful data, there is a lack of near-IR spectra of CH_4 intimately mixed with solid H_2O, as it is likely it will be found on some icy bodies in the outer Solar System.

Since an interaction with H_2O on a molecular level has been shown to cause significant changes in the position and profile of CH_4 absorptions in the mid-IR (e.g., Hudgins et al., 1993), the presence of H_2O could change peaks in the near-IR as well. This would complicate the interpretation of reflection spectra of outer Solar System bodies. In this paper we present near-IR spectra of H_2O–CH_4 ice mixtures at various concentrations and temperatures from 15 to 150 K, and document how peaks shift and broaden, both as a result of interactions with H_2O and as a result of changes in temperature. It is to be hoped that this data will be used, in conjunction with observations, to constrain

* Corresponding author. Fax: +1 650 604 6779.
E-mail address: mbernstein@mail.arc.nasa.gov (M.P. Bernstein).

0019-1035/$ – see front matter
doi:10.1016/j.icarus.2005.10.021

the state of solid CH_4 on the surface of outer Solar System bodies.

2. Materials and methods

The basic techniques and equipment employed for this study have been described previously as part of our mid-IR studies of various compounds in H_2O at low temperature (Hudgins et al., 1993). Details associated with the materials and methods used that are unique to this particular study are provided below. Supplementary and related electronic materials (including additional spectra) are available at our web site, http://www.astrochem.org.

2.1. Experimental procedure

The H_2O was purified via a Millipore Milli-Q water system to 18.2 MΩ and freeze-pump thawed at least three times to remove dissolved gases prior to use. Methane (Matheson UHP = 99.97%) was used without further purification. Samples were pre-mixed at room temperature in volume-calibrated, greaseless glass bulbs and allowed to equilibrate for at least 24 h before use. The background pressure in the gas-handling system was $\sim 10^{-5}$ mbar, compared to total pressures in the sample bulbs of tens of millibar, so the contaminant levels in the bulbs associated with the mixing process were negligible. Bulbs were made of $H_2O/CH_4 = 87$, 20, and 3 mixtures, and of pure CH_4.

Once prepared, glass sample bulbs were transferred to the stainless steel vacuum manifold where the sample mixture was vapor-deposited onto a CsI window cooled to 15 K by an Air Products Displex CSW 202 closed-cycle helium refrigerator. Gas mixtures were deposited first for 10 min against a cold shield before depositing onto the sample window so as to minimize the bias in the ice towards the more volatile component early in the deposit. If this is not done then the first ice that condenses has a higher proportion of CH_4 (a lower H_2O/CH_4 ratio) than in the gas phase in the bulb. We find that this procedure gives a solid sample more representative of the gas-phase mixing ratio in the bulb, but also certainly depends on the substrate temperature. While samples vapor deposited at 15 K (after a delay as described above) have compositions that match the gas-phase mixing ratio in the sample bulb, a $H_2O/CH_4 = 20$ gas mixture that was vapor deposited onto the same substrate at 74 K produced an ice that had an apparent composition closer to $H_2O/CH_4 = 200$, presumably because CH_4 is less likely to condense at higher temperature. Warming to 74 K an ice that was vapor deposited at 15 K does not cause such a dramatic loss of methane (see Fig. 2). IR spectra were measured on a Biorad Excalibur FTS 3000 spectrometer with ambient DTGS and LN_2 cooled MCT detectors and salt and quartz beam splitters that permit measurements in both the mid- and near-infrared.

The mid-IR spectra (i.e., Fig. 1) were measured for ices only tenths of micrometer thick, whereas the others are ∼10 μm thick. H_2O mixtures were deposited at a rate sufficient to produce samples a few tenths of a micrometer thick after a few minutes. Under these conditions the samples are composed of CH_4 in H_2O, mixed at a molecular level. Pure H_2O deposited

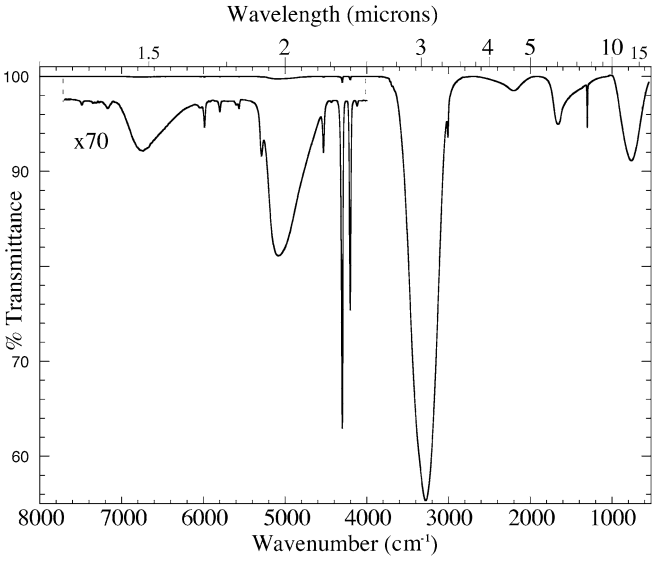

Fig. 1. The 1.25–19.2 μm (8000–520 cm^{-1}) IR spectrum of an $H_2O/CH_4 = 20$ ice mixture at 15 K. The inset shows a (70×)-magnified view of absorptions too weak to be seen in the upper trace, and it has been offset for clarity. The absorptions at ∼1.5, 1.89, ∼2, ∼3, 4.5, ∼6, and 13.3 μm (6700, 5300, 5100, 3250, 2200, 1600, and 750 cm^{-1}) are all caused by solid H_2O. The other sharper features are caused by CH_4, see Table 1.

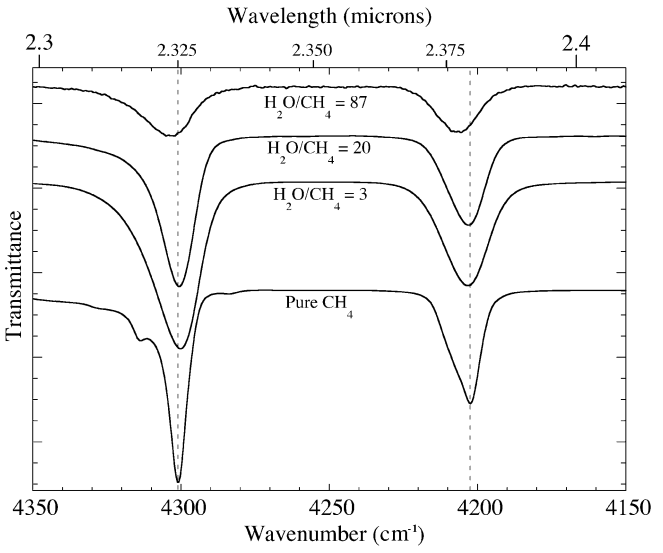

Fig. 2. A comparison of the 2.3–2.4 μm (4350–4150 cm^{-1}) IR spectra of pure methane and three H_2O–CH_4 mixtures at 15 K. The methane absorptions shift to shorter wavelength (higher frequency) and become broader when CH_4 is diluted in H_2O. In addition the relative peak areas also change. Spectra have been offset for clarity.

under these conditions is in its high density amorphous form when deposited at 15 K, and after warming the H_2O goes through several phase transitions (Jenniskens and Blake, 1994; Jenniskens et al., 1995). Clearly, the situation for mixtures is more complex. We do not know the phase of the H_2O in these mixtures but our IR spectra of H_2O/CH_4 mixtures are consistent with previous observations of phases of pure H_2O, so the results described below probably include near-IR spectra of CH_4 in various amorphous and crystalline phases of H_2O ice depending on the temperature. The pure methane film (Fig. 2) was

deposited faster, at a rate that produced a 2-μm thick ice after ∼7 min of deposit.

We note as a caveat that spectra of frosts vapor deposited at low temperature (such as we shall present here) can differ from those of thick ices made by the cooling of higher temperature materials in a closed cell (Quirico and Schmitt, 1997; Section 2). While the closed cell technique provides vastly superior signal to noise spectra for pure ices, there are some cases where it is not applicable. For example, when working with components with very different volatilities (such as is the case here with CH_4 and H_2O) the measurement of ices where the components are mixed as a molecular level would presumably be precluded by preferential condensation of the less volatile component before the more volatile one. In addition, water ice condensed in such a closed cell would presumably form and remain in whatever crystalline phase formed during cool-down, whereas our warm-up and cool down procedure allows us to explore both amorphous and crystalline phases that may be relevant to outer Solar System environments where the H_2O ice is present (Roush, 2001; Hansen and McCord, 2004).

2.2. Peak areas and uncertainties

The areas we report in Table 1 for the near-IR absorptions of CH_4 in H_2O are all normalized relative to the peak near 2.326 μm (4300 cm^{-1}), because we have no absolute scale against which to directly measure true intensities of the peaks. However, we can estimate intrinsic (absolute) absorptivities (A values) of our near-IR absorptions if we accept the A values of mid-IR absorptions of CH_4 in $H_2O/CH_4 = 20$ reported by Hudgins et al. (1993) and ratio the areas of our near-IR CH_4 absorptions to the mid-IR peaks for which A values are known. Given that for an $H_2O/CH_4 = 20$ ice the intrinsic strength of the 3.323 μm (3009 cm^{-1}) C–H stretch of CH_4 is 3.6×10^{-18} cm per molecule, and that of the 7.675 μm (1303 cm^{-1}) C–H wag is 4.7×10^{-18} (Hudgins et al., 1993) then the A values for the two largest near-IR methane peaks at 2.326 and 2.379 μm (4300 and 4203 cm^{-1}) are $2.4(\pm0.4) \times 10^{-19}$, and $1.4(\pm0.3) \times 10^{-19}$, respectively. Thus, the normalized band areas in Table 1 can be converted to absolute A values (at least for the $H_2O/CH_4 = 20$ ice) by multiplying by $\sim 2 \times 10^{-19}$ cm per molecule.

The error reported above (∼20%) is only the scatter from five measurements, and thus reflects the uncertainty in the precision, not the full uncertainty in the accuracy. Since our A values are based on those of Hudgins et al. (1993), who claim an accuracy of no better than a factor of two, we can claim no better.

3. Experimental results

Fig. 1 shows the overall near- and mid-IR spectrum (1.25–19.2 μm; 8000–520 cm^{-1}) of an $H_2O/CH_4 = 20$ solid mixture at 15 K. The inset shows a (70×)-magnified view of absorptions too weak to be seen in the upper trace. The broad strong absorptions at approximately 1.5, 2.0, 3.0, 4.5, 6.0, and 13 μm (6700,

Table 1
Peak positions[a], widths[a], and areas[b] for CH_4 in solid H_2O at 15 K

$H_2O/CH_4 = 87$			$H_2O/CH_4 = 20$			$H_2O/CH_4 = 3$			Pure CH_4		
Position	FWHM	Area[b]	Position	FWHM	Area[b]	Position	FWHM	Area[b]	Position	FWHM	Area[b]
						7485	∼30	2.4×10^{-2}	7487	10	1.3×10^{-2}
						7450–7025		0.29	7360–7260		3.1×10^{-2}
						7167	∼50	See above	7128	10	6.4×10^{-3}
									7083	7	6.8×10^{-3}
									sh 7062		
									sh 6043		
									6032	17	1.4×10^{-2}
						sh 6040			sh 6000		
						5985	18	0.10	5987	8	7.6×10^{-2}
			5984	13	5.2×10^{-2}						
									5919	9	4.0×10^{-3}
			5798	15	3.1×10^{-2}	5800	18	3.4×10^{-2}	5800	8	3.3×10^{-2}
									5595	4	4.0×10^{-3}
									sh 5586		
			sh 5602			sh 5600			sh 5574		
			5564	15	4.0×10^{-2}	5564	14	3.3×10^{-2}	5566	6	2.2×10^{-2}
4532	15	0.1	4529	15	0.15	4530	18	0.12	4528	10	0.12
									sh 4314		
									4301	6	1.0
4304	20	1.0	4301	15	1.0	4300	18	1.0			
4206	14	0.73	4204	12	0.53	4203	16	0.54	4202	10	0.56
						4119	16	1.9×10^{-2}	4115	10	1.7×10^{-2}
						3848	15	4.8×10^{-2}	3848	2	5.5×10^{-2}
									sh 3021		
			3009	10	18	3008	14	17	3009	4	18

[a] All positions and peaks widths (FWHM) are given in wavenumbers.
[b] Peak areas are relative, having been normalized to the CH_4 peak near 4300 cm^{-1} (2.326 μm). The relative numbers can be converted to approximate absolute values (at least for the $H_2O/CH_4 = 20$ ice) by multiplying by $\sim 2 \times 10^{-19}$ cm per molecule. See Section 2.2 for details.

5100, 3250, 2200, 1600, and 750 cm^{-1}) are typical of those observed previously for pure amorphous solid H_2O (Hudgins et al., 1993; Gerakines et al., 2005). Solid H_2O is also responsible for the sharper, weaker, feature near 1.89 μm (5300 cm^{-1}), see discussion for details.

The other, sharp features at 1.671, 1.725, 1.797, 2.208, 2.325, 2.379, 3.323, and 7.68 μm (5984, 5798, 5564, 4529, 4301, 4204, 3009, and 1302 cm^{-1}) are caused by CH_4. The mid-IR absorptions of CH_4 in H_2O have been published previously (Hudgins et al., 1993) but to our knowledge near-IR spectra of H_2O–CH_4 mixtures have not. In Table 1 we summarize the CH_4 absorptions we have observed in frosts of vapor deposited pure CH_4, and three mixtures ($H_2O/CH_4 = 87$, 20, and 3) at 15 K. In general, the absorptions of CH_4 diluted in H_2O are broader and appear at slightly shorter wavelength than in the spectrum of pure CH_4. This, and other observations, will be exemplified in subsequent figures using the two strongest near-IR absorptions of CH_4, the $(\nu_3 + \nu_4)$ and $(\nu_1 + \nu_4)$ combination modes near 2.326 and 2.381 μm (4300 and 4200 cm^{-1}), respectively, as examples.

Peak width and central peak frequency increase with H_2O/CH_4 ratio. This is demonstrated in Fig. 2, where the 2.3–2.4 μm (4350–4150 cm^{-1}) IR spectrum of pure CH_4 is plotted with those of the three H_2O/CH_4 mixtures. The effect is most apparent for the $H_2O/CH_4 = 87$ mixture (top trace, Fig. 2), where the central positions of these two peaks fall short of those in pure CH_4 (lower trace, marked by hatched lines). The $(\nu_3 + \nu_4)$ and $(\nu_1 + \nu_4)$ absorptions of CH_4 in the $H_2O/CH_4 = 87$ mixture are shifted by 1.6×10^{-3} and 2.3×10^{-3} μm (3 and 4 cm^{-1}), respectively, from those in pure solid CH_4 under identical conditions.

In addition to these small shifts in position, these two absorptions in the $H_2O/CH_4 = 87$ mixture are ~3 and 1.5 times broader than those in pure solid CH_4 at the same temperature. As a result, the shoulders evident on the sides of the $(\nu_3 + \nu_4)$ and $(\nu_1 + \nu_4)$ absorptions of pure solid CH_4 are obscured in H_2O/CH_4 mixtures (compare lower and upper spectra in Fig. 2).

The positions, profiles, and relative intensities of CH_4 absorptions in an H_2O/CH_4 mixture depend on temperature as well as concentration. The two strong CH_4 absorptions near 2.325 and 2.380 μm at 15 K are seen in Fig. 3 to (blue) shift and broaden with increasing temperature from 15 to 150 K. The other CH_4 peaks behave in a similar fashion, e.g., the $2\nu_3$ absorption shifts from 1.671 to 1.668 μm (5985 to 5994 cm^{-1}) and the $(\nu_2 + \nu_3 + \nu_4)$ from 1.724 to 1.722 μm (5800 to 5807 cm^{-1}) over the range of 15–150 K (not shown). These temperature-dependent changes are, to a great extent, reversible on re-cooling, despite the fact the phase changes of the H_2O (into which the CH_4 is frozen) are irreversible. These reversible, temperature-dependent, shifts in central position of both the $(\nu_1 + \nu_4)$ and $(\nu_3 + \nu_4)$ combination modes (2.380 and 2.325 μm peaks) are represented graphically in Fig. 4. The rise and fall of the data points makes plain the reversibility of the temperature shift, and the overlap demonstrates that it applies to both peaks (although to different extents). A single experiment where an $H_2O/CH_4 = 20$ mixture was vapor deposited at ~74 K (empty

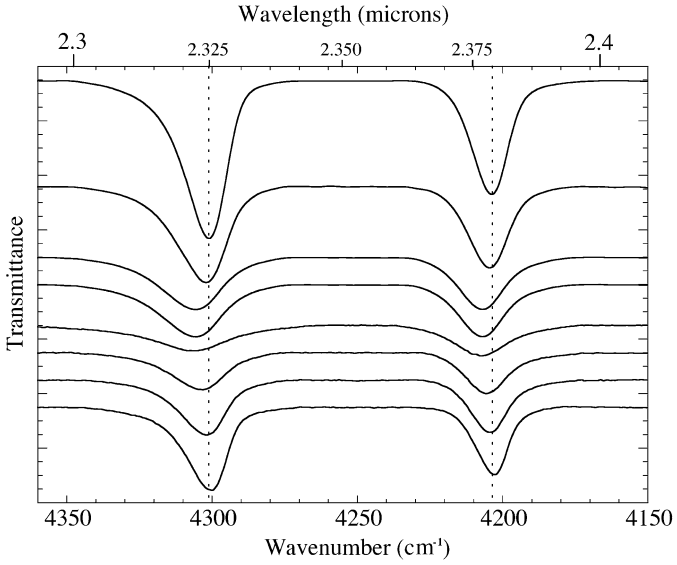

Fig. 3. The 2.3–2.4 μm (4360–4150 cm^{-1}) IR spectra of an $H_2O/CH_4 = 20$ ice mixture at 15 K (top), during warming up to 150 K (middle), and re-cooling back to 30 K (bottom). The temperature-dependent shifts in the position, width, and relative intensity of CH_4 absorptions are reversible on re-cooling (see Figs. 4–6), despite the fact that the phase changes of the water ice are irreversible. The *absolute* intensity never entirely recovers, presumably due to sublimation of CH_4. Spectra have been offset for clarity.

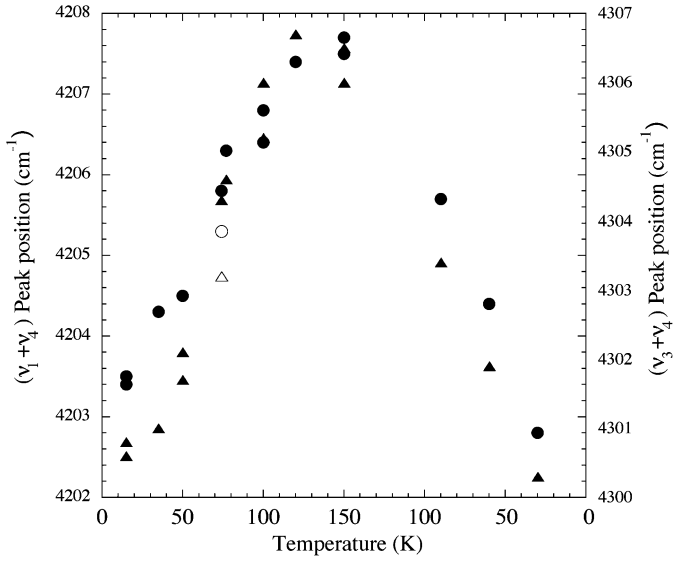

Fig. 4. Peak position vs temperature for the 2.32 and 2.38 μm (4300 and 4200 cm^{-1}; ▲ and ●, respectively) methane absorptions of an $H_2O/CH_4 = 20$ ice. From left to right vapor deposited at 15 K, warmed to 150 K, and then re-cooled to 30 K. The peak positions increase in frequency with increasing temperature, but return to essentially the original values on re-cooling. The empty symbols represent the positions of the same peaks vapor deposited at 74 K.

symbols in Fig. 4) yielded peak positions that were, within uncertainties, consistent with those observed for the ice vapor deposited at 15 K and then warmed. This suggests that peak position depends more on the temperature at the time of observation than at the time of initial deposit.

As can be seen from Fig. 5, the pattern for changes in the peak width vs temperature are very similar to those for peak

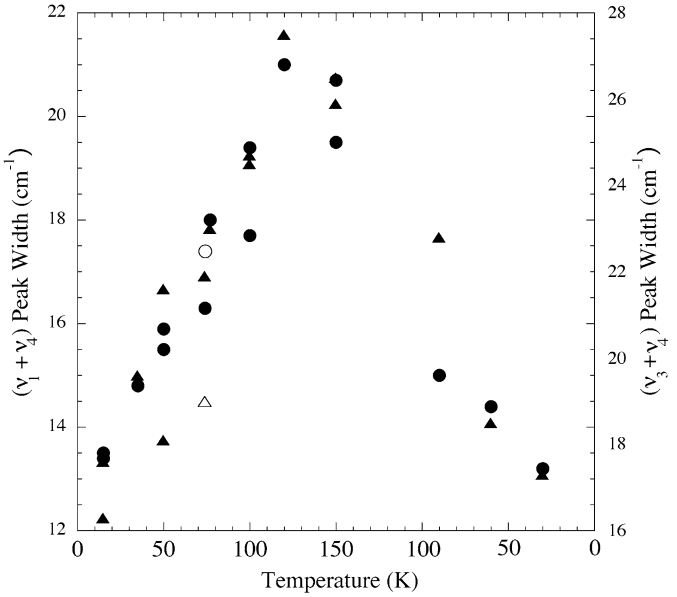

Fig. 5. Peak widths vs temperature for the 2.32 and 2.38 μm (4300 and 4200 cm^{-1}; ▲ and ●, respectively) methane absorptions of an $H_2O/CH_4 = 20$ ice. From left to right vapor deposited at 15 K, warmed to 150 K, and then re-cooled to 30 K. The peak widths increase with increasing temperature, but return to essentially the original values on re-cooling. The empty symbols represent the widths of the same peaks vapor deposited at 74 K.

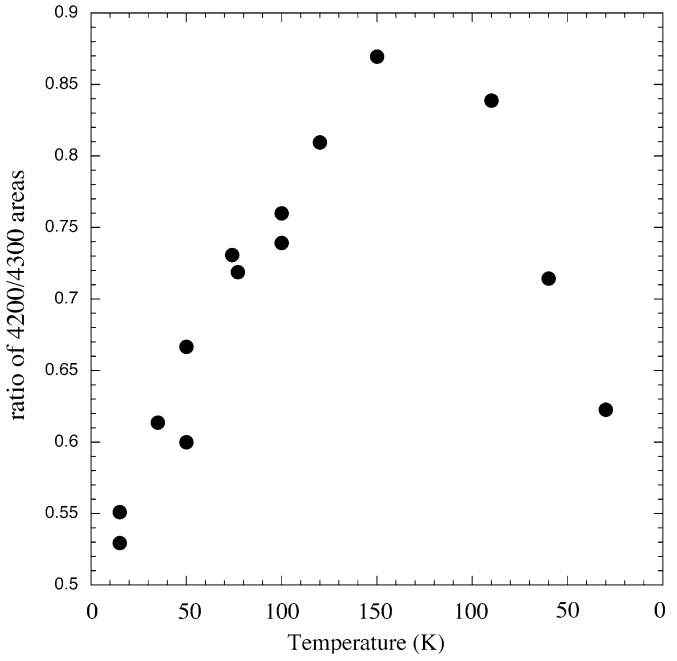

Fig. 6. The ratio of the 2.38/2.32 μm (4200/4300 cm^{-1}) methane absorptions vs temperature for an $H_2O/CH_4 = 20$ ice vapor deposited at 15 K, warmed to 150 K, and then re-cooled to 30 K. Like the position and width, the ratio of areas seems to be reversible with respect to temperature.

position. As before, the effect is reversible, the same pattern for both peaks, and an ice deposited at ∼74 K displays peak widths equivalent to those in the spectra of ices deposited at low temperature and then warmed to 74 K.

The changes in the $(\nu_1+\nu_4)/(\nu_3+\nu_4)$ (i.e., 2.380/2.325 μm) peak area ratio on warming of ices vapor deposited at 15 K seen in Fig. 6 is similar to those seen above for peak position and width. The relative areas of the two main peaks vary reversibly with temperature. However, vapor deposition of an $H_2O/CH_4 = 20$ gas mixture onto a substrate at 74 K produced an ice with a 2.380/2.325 μm peak area ratio very close to one, very much higher than what is observed when an $H_2O/CH_4 = 20$ ice is warmed to 74 K. Vapor deposition of an $H_2O/CH_4 = 20$ mixture at 74 K gave a $H_2O/CH_4 = 200$ ice, ten times more dilute because the CH_4 is less likely to condense at higher temperatures. The 2.380/2.325 μm peak area ratio close to one is expected for a more dilute mixture (see Fig. 2). Thus, the fact that the peak ratio after warming to 74 K differs from that deposited at 15 K and warmed to 74 K is a result of a concentration effect.

At all temperatures the 2.380/2.325 μm peak area ratio for an $H_2O/CH_4 = 20$ mixture is less than one. The longer wavelength peak has less area at all concentrations at 15 K, even for pure CH_4. The reverse (i.e., a 2.380/2.325 μm peak area ratio greater than one) was reported for pure solid CH_4 at 21 K (Quirico and Schmitt, 1997; Table III). However, this is not necessarily inconsistent, since our samples were vapor deposited as a frost at 15 K, whereas theirs were prepared by cool-down of a sample in a closed cell. These very different modes of sample preparation are known to sometimes display spectral differences (see Section 2).

Overall, the peak positions, widths, and relative areas are all temperature sensitive but reversible, despite the fact that these same parameters change irreversibly for the H_2O into which the CH_4 is frozen.

4. Discussion

We have seen that the positions, profiles, and relative areas of CH_4 near-IR absorptions in H_2O differ slightly but significantly from those of pure CH_4. That the near-IR absorptions of CH_4 in H_2O differ, but not radically, from those of pure CH_4 is perhaps not surprising given that CH_4 is a simple hydrocarbon that does not hydrogen bond with H_2O. Thus, while CH_4 (and thus its spectrum) could not but be affected somewhat by the 'matrix' into which it is frozen, there are no dramatic changes of the type that one sees for CO_2 (Bernstein et al., 2005) or molecules that hydrogen bond, such as NH_3 (Schmitt et al., 1998). Nevertheless, it is to be hoped that the combined systematic changes of positions, widths, and relative peak heights recorded here will help observers ascertain whether CH_4 is pure or intimately mixed with H_2O on the surfaces of icy bodies, like Quaoar. Based on the high H_2O/CH_4 ratios in comets (Gibb et al., 2003) one might naively predict the highest dilution mixture to be representative of what would be observed on an outer Solar System object. However, the recently acquired spectra of Kuiper Belt Objects 2003 UB_{313} (Trujillo et al., 2005; Brown et al., 2005) and FY9 (Barkume et al., 2005) were reported to be more consistent with a CH_4-rich H_2O-poor surface.

The differences in positions of these peaks in the spectrum of pure CH_4 vs CH_4 in solid H_2O is reminiscent of what was seen

previously in comparisons of pure CH_4 with CH_4 in solid N_2 (Quirico and Schmitt, 1997). In that case the central positions of the ($\nu_3 + \nu_4$) and ($\nu_1 + \nu_4$) combination modes (at 2.380 and 2.325 μm) of CH_4 in N_2 were, like those of CH_4 in H_2O, shortward of their positions in pure CH_4 (Quirico and Schmitt, 1997; Fig. 7 and Table XI). Thus, the central positions of 2.380 and 2.325 μm peaks of CH_4 in N_2 are closer that of CH_4 in H_2O than to that of pure CH_4. However, out of these three cases the widths are greatest for CH_4 in H_2O, so one should be able to distinguish based on peak profiles.

We have observed the 2.380 and 2.325 μm peaks of CH_4 to shift to higher frequency and increasing width with increasing temperature. These are the same trends that were observed for pure methane (Grundy et al., 2002). We have also noted that ices vapor deposited at 74 K have peak positions and widths equivalent to those deposited at 15 K and then subsequently warmed. These changes with temperature are reversible, despite the fact the phase changes of the H_2O (into which the CH_4 is frozen) are irreversible. This is quite different from the irreversible changes in the spectra of CH_3OH in H_2O (unpublished results), perhaps because CH_3OH forms hydrogen bonds with H_2O, whereas CH_4 does not.

The relative peak areas of the 2.380 and 2.325 μm peaks of CH_4 change with concentration and temperature. For most of our ices the area of the latter absorption (2.325 μm, 4300 cm^{-1}) exceeds the former (2.380 μm, 4200 cm^{-1})—even for pure CH_4—whereas the opposite was observed for pure CH_4 by Quirico and Schmitt (1997). Since their ices were formed at elevated temperature by cooling down a closed cell, and ours were vapor deposited at 15 K, we think that the peak ratio differences between experiments is caused by our very different experimental methods (see Section 2.1). In our most dilute ice deposited at 15 K ($H_2O/CH_4 = 87$), we note that the relative peak areas (and heights) differ significantly from those of pure CH_4 (compare top and bottom traces in Fig. 2).

That the broad peaks of CH_4 in H_2O are still observed at 150 K in the lab reminds us that volatiles such as CH_4 will persist in solid H_2O to much higher temperatures than they would as pure solids. Thus it is possible that an object dominated by water ice might experience a transient heating event that would cause the H_2O to crystallize, and yet CH_4 would remain. Subsequent cooling would leave in a surface with signatures of crystalline H_2O, but CH_4 absorptions with positions, profiles and relative proportions indicative of the final lower temperature (see Figs. 3–6).

The areas of the methane peaks are observed to diminish with increasing temperature. Some of this loss of intensity on warming must be the result of sublimation of CH_4 from the H_2O/CH_4 (= 20) mixture because the features never entirely recover the original intensity they possessed before heating (see Fig. 2). However, sublimation can account for only part of the effect, because after re-cooling the peaks recover some of the lost area, but the experimental design does not allow recondensation of CH_4. Thus, there must be a reversible decrease in intrinsic per-molecule intensity of these CH_4 peaks on warming that could result in an underestimate (of up to a factor of two) in the amount of CH_4 present.

Another interesting feature observed in our H_2O/CH_4 mixtures is the peak at 1.89 μm (∼5300 cm^{-1}) seen in Fig. 1, which may be indicative of amorphous H_2O since it diminishes on warming (see Fig. 3 in Schmitt et al., 1998). We conjecture, based on its position, that this peak may be an overtone combination of two H_2O absorptions, the ∼6.3 μm (∼1600 cm^{-1}) bending mode and the 2.74 μm (3650 cm^{-1}) dangling OH feature, the latter of which is not visible in the figures in this paper, but has been presented elsewhere (Rowland et al., 1991; Bernstein et al., 2005).

5. Summary

1. We have presented the first near-IR spectra of H_2O/CH_4 solid mixtures.
2. The absorptions of CH_4 in H_2O are broader and shifted to higher frequency compared to those of pure solid CH_4 at the same temperature.
3. The absorptions of CH_4 in H_2O become broader, shift to higher frequency, and display changes in relative and absolute intensity with increasing temperature from 15 to 150 K. These changes are reversible on re-cooling, despite the fact the phase changes of the H_2O (into which the CH_4 is frozen) are irreversible.
4. The positions and profiles of peaks vapor deposited at 74 K are equivalent to those deposited at 15 K and then subsequently warmed, but the relative intensities are significantly different because of concentration effects.

Acknowledgments

This work was supported by NASA's Planetary Geology and Geophysics program (NRA-02-OSS-01-PGG). The authors thank Dr. L.J. Allamandola for useful comments and guidance, and the expert technical and experimental support of Robert Walker.

References

Barkume, K.M., Brown, M.E., Schaller, E.L., 2005. Near-infrared spectroscopy of icy planetoids. In: DPS Meeting #37. American Astronomical Society, Abstract 52.11.

Barucci, M.A., Cruikshank, D.P., Dotto, E., Merlin, F., Poulet, F., Dalle Ore, C., Fornasier, S., de Bergh, C., 2005. Is Sedna another Triton? Astron. Astrophys. 439, L1–L4.

Bernstein, M.P., Cruikshank, D.P., Sandford, S.A., 2005. Near-infrared laboratory spectra of solid H_2O/CO_2 and CH_3OH/CO_2 ice mixtures. Icarus 179, 527–534.

Brown, M.E., 2003. The composition of Kuiper belt objects. In: DPS Meeting #35. American Astronomical Society, Abstract 29.01.

Brown, M.E., Trujillo, C.A., Rabinowitz, D., 2005. 2003 EL_61, 2003 UB_313, and 2005 FY_9. In: Green, D.W.E. (Ed.), IAU Circ., vol. 8577, p. 1

Cruikshank, D.P., Apt, J., Brown, R.H., Pilcher, C.B., 1982. Methane on Triton: Physical state and distribution. Bull. Am. Astron. Soc. 14, 765.

Cruikshank, D.P., Pilcher, C.B., Morrison, D., 1976. Pluto—Evidence for methane frost. Science 194, 835–837.

Gerakines, P.A., Bray, J.J., Davis, A., Richey, C.R., 2005. The strengths of near-infrared absorption features relevant to interstellar and planetary ices. Astrophys. J. 620, 1140–1150.

Gibb, E.L., Mumma, M.J., dello Russo, N., Disanti, M.A., Magee-Sauer, K., 2003. Methane in Oort cloud comets. Icarus 165, 391–406.

Grundy, W.M., Buie, M.W., 2001. Distribution and evolution of CH_4, N_2, and CO ices on Pluto's surface: 1995 to 1998. Icarus 153, 248–263.

Grundy, W.M., Schmitt, B., 1998. The temperature-dependent near-infrared absorption spectrum of hexagonal H_2O ice. J. Geophys. Res. 103, 25809–25822.

Grundy, W.M., Schmitt, B., Quirico, E., 2002. The temperature-dependent spectrum of methane ice I between 0.7 and 5 μm and opportunities for near-infrared remote thermometry. Icarus 155, 486–496.

Hansen, G.B., McCord, T.B., 2004. Amorphous and crystalline ice on the Galilean satellites: A balance between thermal and radiolytic processes. J. Geophys. Res. 109 (E1), doi:10.1029/2003JE002149. E01012.

Hudgins, D.M., Sandford, S.A., Allamandola, L.J., Tielens, A.G.G.M., 1993. Mid- and far-infrared spectroscopy of ices, optical constants and integrated absorbances. Astrophys. J. Suppl. Ser. 86, 713–870.

Jenniskens, P., Blake, D.F., 1994. Structural transitions in amorphous water ice and astrophysical implications. Science 265, 753–756.

Jenniskens, P., Blake, D.F., Wilson, M.A., Pohorille, A., 1995. High-density amorphous ice, the frost on interstellar grains. Astrophys. J. 455, 389–401.

Khare, B.N., Thompson, W.R., Sagan, C., Arakawa, E.T., Bruel, C.J., Judish, P., Khanna, R.K., Pollack, J.B., 1989. Optical constants of solid methane. Bull. Am. Astron. Soc. 21, 982.

Pearl, J., Ngoh, M., Ospina, M., Khanna, R., 1991. Optical constants of solid methane and ethane from 10,000 to 450 cm^{-1}. J. Geophys. Res. 96, 17477–17482.

Quirico, E., Schmitt, B., 1997. Near-infrared spectroscopy of simple hydrocarbons and carbon oxides diluted in solid N_2 and as pure ices: Implications for Triton and Pluto. Icarus 127, 354–378.

Quirico, E., Doute, S., Schmitt, B., de Bergh, C., Cruikshank, D.P., Owen, T.C., Geballe, T.R., Roush, T.L., 1999. Composition, physical state, and distribution of ices at the surface of Triton. Icarus 139, 159–178.

Rowland, B., Fisher, M., Devlin, P.J., 1991. Probing icy surfaces with the dangling OH mode absorption: Large ice clusters and microporous amorphous ice. J. Chem. Phys. 95, 1378–1384.

Roush, T.L., 2001. Physical state of ices in the outer Solar System. J. Geophys. Res. 106 (E12), 33315–33324.

Schmitt, B., Quirico, E., Trotta, F., Grundy, W.M., 1998. Optical properties of ices from UV to infrared. In: Schmitt, B., de Bergh, C., Festou, M. (Eds.), Solar System Ices. In: Astrophysics and Space Science Library (ASSL) Series, vol. 227. Kluwer Academic, Dordrecht, pp. 199–240.

Trujillo C.A., Barkume, K.M., Brown, M., Schaller, E.L., Rabinowitz, D.L. 2005. Near-infrared spectra from Mauna Kea of the new brightest Kuiper belt object. In: DPS Meeting #37. American Astronomical Society, Abstract 52.06.